MAGNETIC BIREFRINGENCE OF LIGHT IN IRON GARNETS

R. V. PISAREV, I. G. SINIĬ, N. N. KOLPAKOVA, and Yu. M. YAKOVLEV

Institute of Semiconductors, USSR Academy of Sciences

Submitted November 22, 1970

Zh. Eksp. Teor. Fiz. 60, 2188–2202 (June, 1971)

The effect of magnetization on the optical indicatrix of magnetic crystals is considered phenomenologically. In the general case, magnetization changes cubically symmetric garnets into biaxial garnets and the position of the optical axes depends on the sign and magnitude of the three magnetooptical coefficients ρ_{11}, ρ_{12} and ρ_{44}. Magnetic birefringence in yttrium, samarium, europium, gadolinium, terbium, dysprosium, holmium, erbium and lutecium iron garnets is investigated experimentally at a wavelength $\lambda = 1.15\ \mu$ and at room temperature. The magnitude of magnetooptical anisotropy and the position of the optical axes are determined. Temperature investigations of magnetic birefringence are carried out in yttrium iron garnet (from 77 to 440°K) and in samarium, europium, terbium, dysprosium and holmium iron garnets (from 77 to 295°K). The observed temperature behavior cannot be described by a simple quadratic dependence on magnetization and its description apparently requires allowance for the contribution of separate sublattices to birefringence. It is shown that iron garnets are a peculiar type of tunable optical crystals in which the birefringence magnitude and the position of the optical axes may be varied in broad limits by rotation of the magnetization in the crystal, by synthesis of crystals containing various amounts of paramagnetic ions in the sublattices, and also by temperature variation.

1. INTRODUCTION

THE first to report visual observation of birefringence of light in iron garnets (chemical formula of the type $X_3Fe_5O_{12}$) was Dillon[1]. The birefringence was revealed by the contrast between domains magnetized in different directions in the plane of a crystal plate on which light was normally incident. Later papers[2,3] reported measurements of magnetic birefringence or the Cotton-Mouton effect in a number of iron garnets.

The birefringence observed in garnets and also in a number of other crystals with different magnetic structures[2] is quite large, $\Delta n \sim 10^{-5}$–10^{-3}. An investigation of this phenomenon in magnetically-ordered crystals is of considerable interest, since it makes it possible to relate the optical and magnetic characteristics of the crystals. Establishment of such a relation is important for the study of the spin dependence of the polarizability of crystals. Such a relation can be used extensively for the study, by optical methods, of the magnetic structure of crystals, the magnetizations of sublattices, magnetic phase transitions, and other phenomena.

We note that investigations of the Cotton-Mouton effect in paramagnets have recently attracted considerable interest[4].

We present here a phenomenological analysis of the deformation of the optical indicatrix of cubic crystals under the influence of magnetization, present the main formulas describing the birefringence of light propagating along the principal crystallographic directions, and consider the positions of the optical axes as functions of the relations between the magnetooptical coefficients. The experimental part of the paper is connected with investigations of birefringence in yttrium and rare-earth iron garnets with the magnetization oriented along different crystallographic directions. In addition to room-temperature data, results of temperature-dependence investigations will be presented for certain crystals. These investigations have revealed great variability in the temperature behavior of birefringence.

2. DEFORMATION OF OPTICAL INDICATRIX UNDER THE INFLUENCE OF MAGNETIZATION

Polarized light propagating along an arbitrary direction in a magnetically ordered crystal should experience a change in its state of polarization. This change is connected with the fact that any magnetically ordered crystal, even if it is cubic from the point of view of crystallographic symmetry, such as ferrites with garnet or spinel structure, is an optically anisotropic medium. The optical anisotropy may be connected with a lower than cubic symmetry of the crystal, which leads to a natural birefringence, with magnetic circular and linear birefringence arising in the presence of a spontaneous ferromagnetic or antiferromagnetic moment[5], and birefringence due to magnetostriction deformations.

We shall analyze the propagation of light within the framework of the concept of the optical indicatrix of a crystal[6,7], the equation of which can be written in an arbitrary coordinate frame in the form

$$B_{ij}x_ix_j = 1, \tag{1}$$

and in the particular case of a cubic crystal in the form

$$B_0(x_1^2 + x_2^2 + x_3^2) = 1, \tag{2}$$

where $B_0 = 1/n_0^2$ and n_0 is the refractive index.

Equation (2) describes the optical indicatrix of a cubic crystal without allowance for magnetic ordering. The change of the refractive indices connected with the presence of spontaneous magnetic ordering is identical with the change of the shape, dimension, and orientation of the optical indicatrix. In the general case, for

arbitrary orientation of the magnetization, the equation of the indicatrix takes the form

$$B_1x_1^2 + B_2x_2^2 + B_3x_3^2 + 2B_4x_1x_2 + 2B_5x_2x_3 + 2B_6x_1x_3 = 1, \quad (3)$$

where the system of contraction of the number of indices is used[8].

The change of the coefficients ΔB_{ij} under the influence of the magnetization can be obtained by solving the matrix equation

$$\Delta B_{ij} = \rho_{ijkl}M_kM_l = \rho_{ijkl}\alpha_k\alpha_l M^2. \quad (4)$$

In cubic crystals, the tensor ρ_{ijkl} has only three nonzero components, $\rho_{1111} = \rho_{11}$, $\rho_{1122} = \rho_{12}$ and $\rho_{4444} = \rho_{44}$[8,9]. The expanded form of (4) is

$$\begin{bmatrix}\Delta B_1\\ \Delta B_2\\ \Delta B_3\\ \Delta B_4\\ \Delta B_5\\ \Delta B_6\end{bmatrix} = \begin{bmatrix}B_1 - B_0\\ B_2 - B_0\\ B_3 - B_0\\ B_4\\ B_5\\ B_6\end{bmatrix} = \begin{bmatrix}\rho_{11} & \rho_{12} & \rho_{12} & 0 & 0 & 0\\ \rho_{12} & \rho_{11} & \rho_{12} & 0 & 0 & 0\\ \rho_{12} & \rho_{12} & \rho_{11} & 0 & 0 & 0\\ 0 & 0 & 0 & 2\rho_{44} & 0 & 0\\ 0 & 0 & 0 & 0 & 2\rho_{44} & 0\\ 0 & 0 & 0 & 0 & 0 & 2\rho_{44}\end{bmatrix}\begin{bmatrix}\alpha_1^2\\ \alpha_2^2\\ \alpha_3^2\\ \alpha_1\alpha_2\\ \alpha_2\alpha_3\\ \alpha_1\alpha_3\end{bmatrix} M^2 \quad (5)$$

$$= \begin{bmatrix}\rho_{11}\alpha_1^2 + \rho_{12}\alpha_2^2 + \rho_{12}\alpha_3^2\\ \rho_{12}\alpha_1^2 + \rho_{11}\alpha_2^2 + \rho_{12}\alpha_3^2\\ \rho_{12}\alpha_1^2 + \rho_{12}\alpha_2^2 + \rho_{11}\alpha_3^2\\ 2\rho_{44}\alpha_1\alpha_2\\ 2\rho_{44}\alpha_2\alpha_3\\ 2\rho_{44}\alpha_1\alpha_3\end{bmatrix} M^2.$$

The equation of the indicatrix has been written out with only the terms quadratic in the magnetization taken into account, i.e., it should describe only effects of birefringence of light. However, the presence of spontaneous magnetic ordering should lead to gyrotropic phenomena, which are linear in the magnetization. In the present paper we shall consider only birefringence effects, i.e., we shall analyze the phenomena occurring with light propagating perpendicular to the magnetization, when the gyrotropy vanishes.

Let us analyze the main cases of birefringence for magnetization directed along the principal crystallographic directions of a cubic crystal.

2.1. $\mathbf{M} \parallel [001]$ (Fig. 1a). In this case the change of the principal refractive indices of the deformed indicatrix is

$$\Delta n_{\parallel} = \Delta n_{001} = -\tfrac{1}{2}n_0^3\rho_{11}M^2,$$
$$\Delta n_{\perp} = \Delta n_{100} = \Delta n_{010} = -\tfrac{1}{2}n_0^3\rho_{12}M^2. \quad (6)$$

It follows therefore that the birefringence for a light beam propagating in the [100] or [010] direction is given by

$$\Delta n = n_{\parallel} - n_{\perp} = -\tfrac{1}{2}n_0^3(\rho_{11} - \rho_{12})M^2. \quad (7)$$

A similar result is obtained when light propagates along any direction in the (001) plane perpendicular to the magnetization. In this case, the magnetization causes the cubic crystal to change from an optically isotropic one into a uniaxial crystal, and the direction of the optical axis coincides with the direction of the magnetization.

2.2. $\mathbf{M} \parallel [111]$ (Fig. 1b). The changes of the refractive indices in the magnetization direction Δn_{111} and for any direction perpendicular to [111], for example Δn_{011}, are

$$\Delta n_{\parallel} = \Delta n_{111} = -\tfrac{1}{6}n_0^3(\rho_{11} + 2\rho_{12} + 4\rho_{44})M^2,$$
$$\Delta n_{\perp} = \Delta n_{011} = -\tfrac{1}{6}n_0^3(\rho_{11} + 2\rho_{12} - 2\rho_{44})M^2, \quad (8)$$

and the birefringence for light propagating perpendicular to [111] is given by

$$\Delta n = n_{\parallel} - n_{\perp} = -n_0^3\rho_{44}M^2. \quad (9)$$

Just as in case 2.1, for such an orientation of the magnetization the optically isotropic crystal becomes uniaxial with the optical axis along the magnetization.

2.3. $\mathbf{M} \parallel [110]$ (Fig. 1c). The principal refractive indices of the indicatrix are changed in the following manner:

$$\Delta n_{110} = -\tfrac{1}{4}n_0^3(\rho_{11} + \rho_{12} + 2\rho_{44})M^2,$$
$$\Delta n_{1\bar{1}0} = -\tfrac{1}{4}n_0^3(\rho_{11} + \rho_{12} - 2\rho_{44})M^2,$$
$$\Delta n_{001} = -\tfrac{1}{2}n_0^3\rho_{12}M^2. \quad (10)$$

The birefringences for light beams propagating along the directions [001] and $[1\bar{1}0]$ are given by different formulas:

$$\mathbf{k} \parallel [001], \quad \Delta n = n_{\parallel} - n_{\perp} = -n_0^3\rho_{44}M^2, \quad (11)$$

$$\mathbf{k} \parallel [1\bar{1}0], \quad \Delta n = n_{\parallel} - n_{\perp} = -\tfrac{1}{4}n_0^3(\rho_{11} - \rho_{12} + 2\rho_{44})M^2, \quad (12)$$

i.e., unlike in cases 2.1 and 2.2, the crystal becomes optically biaxial.

To describe the optical behavior of cubic crystals under the influence of magnetization, it is convenient to introduce the ratio of the birefringence values in the two principal cases 2.1 and 2.2, namely the ratio

$$a = \frac{2\rho_{44}}{\rho_{11} - \rho_{12}}, \quad (13)$$

which describes the magnetooptical anisotropy. If a = 1, then it follows from (7), (9), (11), and (12) that at any orientation of the magnetization in the crystal the birefringence will have the same value, i.e., the birefringence will be isotropic. In this case the crystal will be optically uniaxial, with an axis directed along the magnetization. If $a \neq 1$, then the crystal will be magnetooptically anisotropic, and magnetization will transform it into an optically biaxial crystal, with the positions of the optical axes dependent on the sign and magnitude of the ratio (13). It is interesting to note that if $a \neq 1$, then the birefringence will be observed also when the light propagates along the magnetization (in addition to the particular cases 2.1 and 2.2), which leads, in conjunction with the longitudinal Faraday effect, to gyroanisotropy of the medium. Experimental observation of this effect in terbium iron garnet was reported in[10].

We present here a formula describing the birefringence of light passing through a plate of a cubic crystal magnetized in its own plane. Let the direction

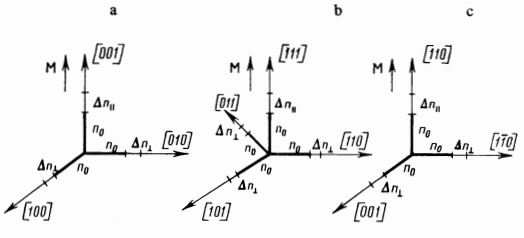

FIG. 1. Main cases of orientation of magnetization in a cubic crystal and variation of the refractive indices: a–$\mathbf{M} \parallel [001]$: $\Delta n_{\parallel} = \Delta n_{001}$, $\Delta n_{\perp} = \Delta n_{100} = \Delta n_{010}$; b–$\mathbf{M} \parallel [111]$: $\Delta n_{\parallel} = \Delta n_{111}$, $\Delta n_{\perp} = \Delta n_{101} = \Delta n_{110} = \Delta n_{011}$; c–$\mathbf{M} \parallel [110]$: $\Delta n_{\parallel} = \Delta n_{110}$, $\Delta n_{001} \neq \Delta n_{110}$.

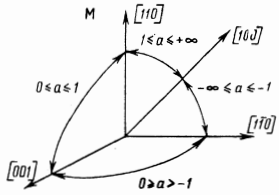

FIG. 2. Position of optical axes in a cubic crystal when the magnetization is oriented along the two-fold axis at different values of the magnetooptical-anisotropy parameter a.

cosines α_i determine the orientation of the magnetization relative to the crystallographic axes. By definition, the direction of propagation of light **k** is perpendicular to the magnetization. Another direction of importance for birefringence is the one perpendicular to the magnetization and to the light beam. We define this direction by the direction cosines β_i. Obviously, by the same token we have defined any direction lying in the plane perpendicular to the magnetization. We have for the birefringence

$$\Delta n = n_\parallel - n_\perp = {}^1/_2 (n_0)^3 M^2 [(\rho_{11} - \rho_{12})(\alpha_1^4 + \alpha_2^4 + \alpha_3^4 - \alpha_1^2\beta_1^2 - \alpha_2^2\beta_2^2 - \alpha_3^2\beta_3^2) + 2\rho_{44}(\alpha_1^2\alpha_2^2 + \alpha_1^2\alpha_3^2 + \alpha_2^2\alpha_3^2 - \alpha_1\alpha_2\beta_1\beta_2 - \alpha_2\alpha_3\beta_2\beta_3 - \alpha_1\alpha_3\beta_1\beta_3)]. \quad (14)$$

3. POSITION OF OPTICAL AXES IN MAGNETIC CRYSTAL

As noted above, a cubic crystal becomes in the general case biaxial under the influence of magnetization. Only if the magnetization is oriented along the high-symmetry directions (the edges and diagonals of the cube), and also if the condition for optical isotropy is satisfied, is the crystal uniaxial with optical axis along the magnetization. In all other cases, the position of the optical axes is determined by the ratio of the coefficients $\rho_{11} - \rho_{12}$ and ρ_{44}. This position can be determined from the condition [6,11]

$$\operatorname{tg} V = [(n_m - n_p) / (n_g - n_m)]^{1/2}, \quad (15)$$

where V is the angle between the optical axis and the magnetization direction, and n_g, n_m, and n_p are respectively the largest, medium, and smallest principal refractive indices. By definition, the optical axes always lie in the plane of the indicatrix with ellipse semiaxes n_g and n_p.

Let us analyze the positions of the optical axes, directing the magnetization along the two-fold axis, **M** ∥ [110] (Fig. 2). We break up the possible cases in accord with the values of the parameter of the magneto-optic anisotropy a.

3.1. $1 \leq |a| \leq \infty$ (Fig. 2). We assume that $0 \leq \rho_{11} - \rho_{12} \leq 2\rho_{44}$; we then obtain from (10) $n_g = n_{1\bar{1}0}$, $n_m = n_{001}$, $n_p = n_{110}$ and, using (15), we have

$$\pm \operatorname{tg} V = \sqrt{\frac{(\rho_{11} - \rho_{12} - 2\rho_{44})(-1)}{\rho_{11} - \rho_{12} + 2\rho_{44}}} = \sqrt{\frac{a-1}{a+1}}, \quad (16)$$

where a is the parameter of the magnetooptical anisotropy, and the angle is reckoned from the direction of the magnetization in the (001) plane. When a = +1, the optical axis is directed along the magnetization, and at a = −1 it is perpendicular to the magnetization along the $[1\bar{1}0]$ axis. At $a = \pm\infty$, the optical axes make an angle of 45° with the magnetization, i.e., they lie along the mutually perpendicular fourfold [100] and [010] axes.

3.2. $0 \leq a \leq 1$ (Fig. 2). Using (10) and (15), we get

$$\pm \operatorname{tg} V = \sqrt{\frac{\rho_{11} - \rho_{12} - 2\rho_{44}}{4\rho_{44}}} = \sqrt{\frac{1-a}{2a}}, \quad (17)$$

where the angle is reckoned from the direction of the magnetization in the $(1\bar{1}0)$ plane. At a = 1 the optical axis lies along the magnetization, and at a = 0 it is perpendicular to the magnetization along [001].

3.3. $0 \geq a \geq -1$ (Fig. 2). When this condition is satisfied, the optical axes lie in the (110) plane and the angle between the optical axis and the $[1\bar{1}0]$ direction can be determined from the formula

$$\pm \operatorname{tg} V = \sqrt{\frac{\rho_{11} - \rho_{12} + 2\rho_{44}}{-4\rho_{44}}} = \sqrt{\frac{-1-a}{2a}}. \quad (18)$$

When a = 0, the optical axis coincides with the [001] direction, and at a = −1 it coincides with the $[1\bar{1}0]$ direction.

When the magnetization swings from the [110] direction to another direction, say [001] or [111], the angle between the optical axes decreases and vanishes when the magnetization coincides with these directions (at all values of a).

4. METHODOLOGICAL REMARKS

The experimental investigation of the birefringence was carried out with the setup described in [2]. The investigations were made at helium-neon-laser wavelengths $\lambda = 1.15\ \mu$ and $3.39\ \mu$ in fields up to 24 kOe. The phase difference between the two waves passing through the sample was registered, just as in [2], with a compensator, and also with a quarter-wave mica plate.

We investigated in the experiments plates of garnet single crystals cut in the principal crystallographic planes (100) (110), and (111). The samples were oriented relative to the developed crystallographic faces and by x-ray diffraction. The sample thickness, depending on the crystal transparency, ranged from 0.5 to 5 mm. To eliminate errors in the determination of the birefringence due to inaccurate setting of the crystals, we measured the birefringence at different orientations of the magnetization in the plane of the sample, by rotating the crystal around the light propagation direction. When using formula (14), such curves made it possible to monitor the correctness of the preliminary orientation and to obtain more reliable values of the birefringence.

The investigations have shown that, in spite of the fact that the garnets are cubic, many samples exhibit strong birefringence in the absence of an external magnetic field. By way of an example, Fig. 3 shows

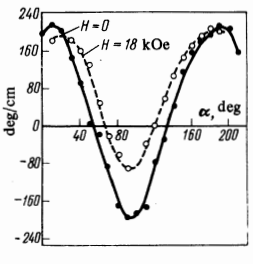

FIG. 3. Birefringence of light in one sample of dysprosium iron garnet in the absence and in the presence of a magnetic field in the (110) plane; T = 295°K, $\lambda = 1.15\ \mu$.

the birefringence of one sample of dysprosium iron garnet in the absence and in the presence of a magnetic field. The reason for such a strong birefringence of certain samples is still unclear. It cannot be connected with crystallographic stresses or with an asymmetrical domain structure. Most samples on which measurements were made revealed no birefringence in the absence of an external field.

In Fig. 3 and further in this article, the birefringence is expressed in terms of the phase difference acquired by two linearly polarized waves after passing through a crystal 1 cm thick. The phase difference β is connected with the difference between the refractive indices by the relation

$$\beta = 2\pi(n_{\parallel} - n_{\perp})/\lambda,$$

where λ is the wavelength of the light.

The temperature dependences of the birefringence were investigated in a cryostat cooled to 77°K at a fixed position of the crystals.

Table I. Magnetic birefringence of iron garnets at T = 295° K, λ = 1.15 μ, and H = 20 kOe

Crystal	H ∥ [100]		H ∥ [111]	
	Δn	β, deg/cm	Δn	β, deg/cm
$Y_3Fe_5O_{12}$	3.87	120	5.16	160
$Y_3Fe_{4.3}Ga_{0.7}O_{12}$	1.6	50	2.88	90
$Sm_3Fe_5O_{12}$	8.06	250	5.00	155
$Eu_3Fe_5O_{12}$	10.25	320	10.00	312
$Gd_3Fe_5O_{12}$	4.00	124	5.1	160
$Tb_3Fe_5O_{12}$	1.44	45	3.8	115
$Dy_3Fe_5O_{12}$	0.97	30	3.55	110
$Ho_3Fe_5O_{12}$	2.72	85	5.0	155
$Er_3Fe_5O_{12}$	3.55	110	5.4	167
$Lu_3Fe_5O_{12}$	3.2	100	5.3	165

5. MAGNETIC BIREFRINGENCE OF GARNETS

Table I gives the results on the magnetic birefringence of all the investigated iron garnets. The table lists the refractive-index difference $\Delta n = n_{\parallel} - n_{\perp}$ (in units of 10^{-5}) and the phase difference β. Figure 4 illustrates cases where the birefringence was measured while rotating certain garnets about the direction of light propagation in the (110) and (100) planes. The solid curves were calculated in accordance with formula (14).

It is interesting to note that the maximum value of the birefringence is observed when the magnetization is oriented in the (110) plane at an angle of approximately 50° to the [100] direction, and when $\mathbf{M} \parallel [111]$ the birefringence turns out to be somewhat smaller (about 5%) (Figs. 4a, b, c). When the magnetization is rotated in the (100) plane (Fig. 4d), the birefringence at the extremal points is proportional to $(\rho_{11} - \rho_{12})$ and $2\rho_{44}$ according to (7) and (11).

At room temperature, as seen from Table I, all the garnets can be subdivided, in accordance with their birefringence, into two groups, with $a > 1$ and $a < 1$ (Table II). The case $a < 1$ is realized in the samarium and europium iron garnets (Fig. 4c). The value of a increases on going from $Sm_3Fe_5O_{12}$ to $Eu_3Fe_5O_{12}$, i.e., as the 4f shell becomes filled. Starting with $Gd_3Fe_5O_{12}$ and beyond, we have $a > 1$, and a certain correlation is observed between the value of a and the effective magnetic moment of the trivalent rare-earth irons.

The closest to being optically isotropic crystals ($a = 1$) are europium iron garnets. The strongest deviation of the parameter a from unity is observed for dysprosium iron garnet. For yttrium iron garnet, a = 1.335. The magnetooptical anisotropy increases to

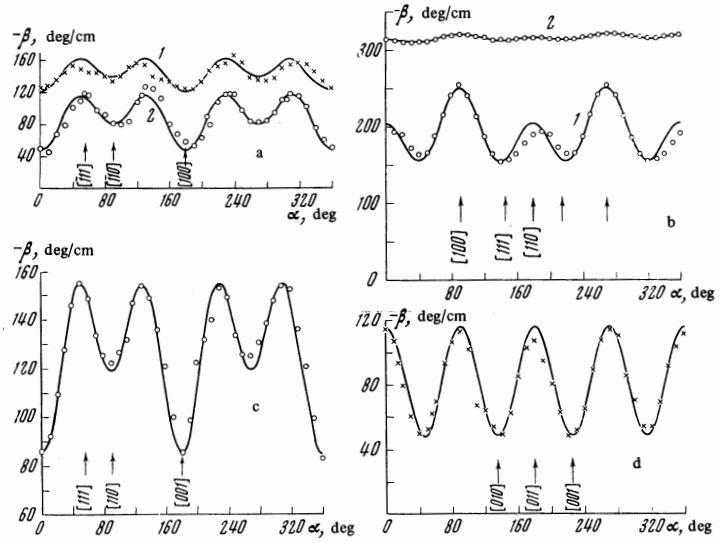

FIG. 4. Magnetic birefringence of light in yttrium (1) and terbium (2) iron garnets (a), in holmium iron garnet (b), and in samarium (1) and europium (2) iron garnets (c) with rotation of the magnetization in the (110) plane. T = 295°K, λ = 1.15 μ, H = 17 kOe, $\mathbf{k} \parallel [110]$; magnetic birefringence of light in terbium iron garnet (d) with rotation of the magnetization in the (100) plane. T = 295°K, λ = 1,15 μ, H = 16.5 kOe, $\mathbf{k} \parallel [110]$.

Table II. Magnetooptical anisotropy a and the angle between the magnetization and the optical axis for the investigated garnets

Crystal	a	V	Crystal	a	V
$Y_3Fe_5O_{12}$	1.335	20°40′	$Tb_3Fe_5O_{12}$	2.67	34°
$Y_3Fe_{4.3}Ga_{0.7}O_{12}$	1.80	28°5′	$Dy_3Fe_5O_{12}$	3.67	37°8′
$Sm_3Fe_5O_{12}$	0.62	28°55′	$Ho_3Fe_5O_{12}$	1.825	28°20′
$Eu_3Fe_5O_{12}$	0.975	6°30′	$Er_3Fe_5O_{12}$	1.52	25°40′
$Gd_3Fe_5O_{12}$	1.29	19°35′	$Lu_3Fe_5O_{12}$	1.65	26°22′

a = 1.80 when the iron ions in the tetrahedral sublattice are partially replaced by gallium ions.

We note that the ratio analogous to (13) for the elastic constants in yttrium iron garnets is 0.95, i.e., the crystal is elastically isotropic with accuracy 5%[12]. The analogous ratio for the photoelastic constants equals 1.8[13].

Table II gives, besides the parameter a, also the angle of inclination of the optical axis to the magnetization, if the latter is directed along a two-fold axis.

A study of the birefringence of the garnets at the wavelength $\lambda = 3.39\ \mu$ has revealed a small decrease of the effect compared with the wavelength $\lambda = 1.15\ \mu$.

Recently, Dillon and co-workers[14] reported the results of measurements of magnetic birefringence in yttrium and rare-earth iron garnets at room temperature and at 77°K for two principal orientations of the magnetization along [100] and [111]. For a number of crystals (yttrium, europium, samarium, gadolinium, and holmium iron garnets) our data at room temperature either coincide with the results of[14] or differ slightly (by not more than 10—15%). For terbium, dysprosium, and erbium iron garnets, the discrepancy between the values of the birefringence is appreciable. For example, for $Dy_3Fe_5O_{12}$ the disparity between the data of Table I and[14] reaches 200%. It should be noted that such a situation is characteristic of room temperature, where the birefringence due to the imperfection of the crystal may be comparable with magnetic birefringence (see the curve for $Dy_3Fe_5O_{12}$ in Fig. 3). At low temperatures, when the magnetic birefringence becomes predominant, the data of the present paper are in much better agreement with[14]. For example, for

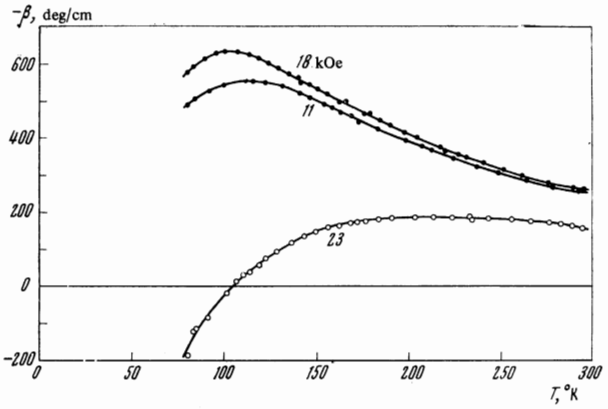

FIG. 6. Temperature dependence of magnetic birefringence in samarium iron garnet with the external field oriented along the principal crystallographic directions in the (110) plane. The light circles and dots denote the same as in Fig. 5.

the same $Dy_3Fe_5O_{12}$ crystal at 77°K, the birefringence as given by the two papers is practically the same. It should be noted that the strong temperature and field dependences of the birefringence at low temperatures require strictly identical experimental conditions when the results are compared.

6. TEMPERATURE AND FIELD DEPENDENCES OF BIREFRINGENCE

Yttrium iron garnet. The temperature dependence of the birefringence at $\mathbf{M} \parallel [100]$ and $\mathbf{k} \perp \mathbf{M}$ was investigated for this crystal in the interval 77—440°K in a field 16 kOe. Figure 5 shows the temperature dependence obtained as a result of averaging several measurements. The temperature dependence of the product of the magnetization of the octahedral and tetrahedral sublattices of $Y_3Fe_5O_{12}$[15,16] was also calculated. Comparison, in relative units, has shown that at low temperatures this curve coincides with that of the birefringence, but the curves diverge starting already approximately at 200°K, and the birefringence decreases more rapidly than the product of the magnetizations. Better agreement can be obtained by taking additional account of the contribution of the octa-

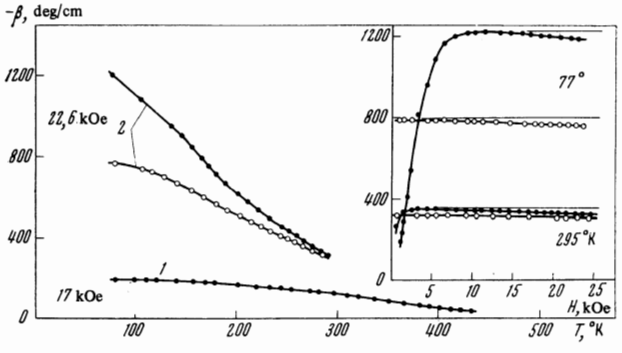

FIG. 5. Temperature dependence of the magnetic birefringence in yttrium (1) and europium (2) iron garnets. Insert—field dependences for $Eu_3Fe_5O_{12}$ (the horizontal lines show that the birefringence decreases with increasing field). All the curves were measured at $\lambda = 1.15\ \mu$. The dark dots correspond to orientation of the external field along [001], and the light circles to orientation along [111].

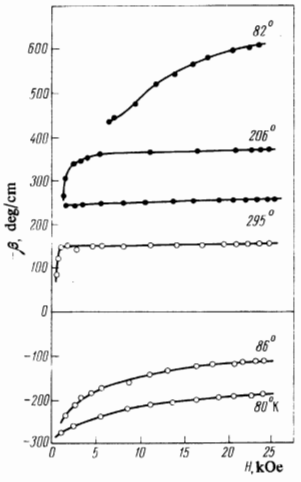

FIG. 7. Dependence of magnetic birefringence on the external field in the (110) plane in samarium iron garnet at different temperatures. The light circles and dots denote the same as in Fig. 5.

hedral and tetrahedral sublattices to the birefringence, which is proportional to the square of the magnetization.

Samarium iron garnet. The results of an investigation of the temperature and field dependences of the birefringence are shown in Figs. 6 and 7. In the case when the magnetization is oriented along the difficult direction, the lowering of the temperature first leads to a growth of the birefringence, but a decrease of the effect is observed at low temperatures. If the magnetization is directed along the easy axis, then the decrease of the birefringence is observed already at 150°K, and in the region of 100°K the effect reverses sign. The dependence of the magnetic birefringence on the external field at low temperatures has an unusual character. Unlike the other investigated iron garnets, the relative change of the birefringence with increasing field is different for $\mathbf{H} \parallel [100]$ and $\mathbf{H} \parallel [111]$. In the former case, the effect increases, and in the latter it decreases. These phenomena can be connected with the strong growth of the magnetic-anisotropy energy[17] or with the relative change of the contribution made to the birefringence by the orbital and spin moments of the samarium sublattice[18].

We note also that the paraprocess in the samarium sublattice at room temperature leads to an increase of the effect with increasing field (both for $\mathbf{H} \parallel [100]$ and $\mathbf{H} \parallel [111]$). Comparison with $Y_3Fe_5O_{12}$ shows that the contribution of the samarium sublattice to the general birefringence turns out to be noticeably larger than the contribution to the magnetization (approximately 0.42 μ_B at T = 0°K with a total magnetization of the samarium iron garnet 5.43 μ_B[16]).

Europium iron garnet. In this crystal the contribution of the europium sublattice to the birefringence is likewise much stronger than the contribution of the summary iron sublattice, in spite of the small moment of the europium ion in the garnet[15,16]. At room temperature, $Eu_3Fe_5O_{12}$ exhibits the largest Cotton-Mouton effect among all the garnets (Table I). Lowering the temperature leads to a growth of the birefringence, which is different for the two magnetization orientations (Fig. 5). The insert of Fig. 5 shows the field dependence of the birefringence at room and nitrogen temperatures. In strong fields, a small decrease of the effect is observed with increasing field. Obviously, this decrease should be attributed to the demagnetization of the europium sublattice with increasing field, since this sublattice is oriented opposite to the summary iron sublattice.

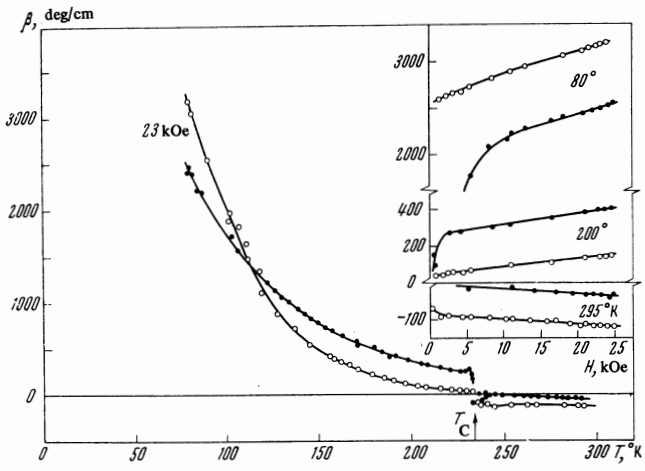

FIG. 9. Temperature dependence and field dependence (insert) of the magnetic birefringence in dysprosium iron garnet. The light circles and dots represent the orientations of the external field in the (110) plane along [111] and [001], respectively.

Terbium iron garnet. The temperature dependence of magnetic birefringence for the principal crystallographic directions, shown in Fig. 8, differs somewhat from the previously published data[2]. The discrepancy can be attributed to the presence of residual birefringence in the previously investigated sample.

Dysprosium iron garnet. The temperature and field dependences for the difficult and easy magnetization directions are shown in Fig. 9. For all the directions, a growth of birefringence is observed with decreasing

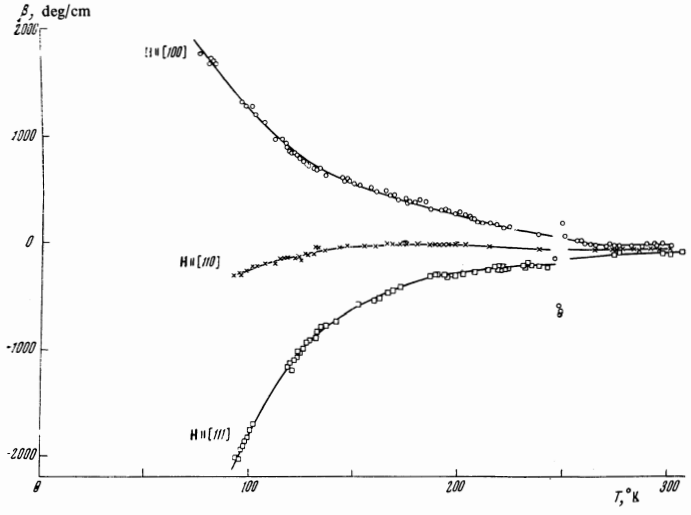

FIG. 8. Temperature dependence of the magnetic birefringence in terbium iron garnets in the (110) plane with the magnetization oriented along the principal crystallographic directions.

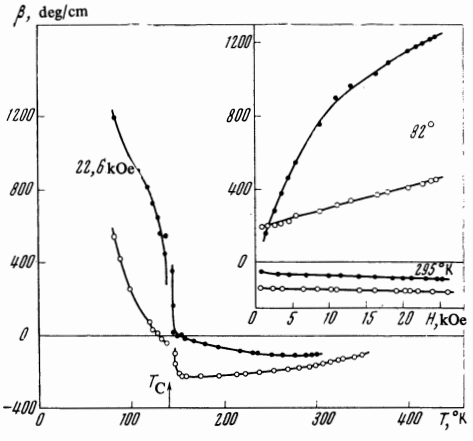

FIG. 10. Temperature dependence and field dependence (insert) of magnetic birefringence in holmium iron garnet. The symbols are the same as in Fig. 9.

temperature, but the growth is not exactly the same. At 295°K we have $\Delta n(\mathbf{H} \parallel [100]) > \Delta n(\mathbf{H} \parallel [111])$, and in the region of the magnetization compensation point the effect for these directions reverses sign, after which the curves intersect, so that at nitrogen temperature we have $\Delta n(\mathbf{H} \parallel [111]) > \Delta n(\mathbf{H} \parallel [100])$. This process is clearly illustrated by the field dependences at different temperatures, shown in the insert of Fig. 9. The compensation point $T_c = 234°K$ turned out to be higher than in[15,16], where $T_c = 226°K$. In the other investigated sample, the compensation temperature was 219°K. The passage through the compensation point is accompanied by a change not only in the sign of the effect but also in the slopes of the plots of the birefringence against the external fields. The slopes of the curves, as in the other garnets, are obviously connected with the paraprocess in the rare-earth sublattice, and the change of slope is connected with the reorientation of the magnetizations of the dysprosium and the summary iron sublattices at the compensation point.

Holmium iron garnet. The results of the investigation of the temperature and field dependences at $\mathbf{H} \parallel [100]$ and $\mathbf{H} \parallel [111]$ are shown in Fig. 10. Lowering the temperature leads to a growth of the birefringence with a reversal of the sign in the region of the compensation point. The anomaly observed in terbium[2] and dysprosium (Fig. 9) iron garnets on going through T_c is even more strongly pronounced in this case, especially when the external field is oriented along the difficult direction. At room temperature, the birefringence increases somewhat with increasing external field (insert of Fig. 10). At nitrogen temperature, the field dependences reveal no saturation and do not become linear, making it difficult to determine the birefringence connected with the spontaneous magnetization.

The results of the temperature investigations show that the magnetic birefringence can change with temperature in a variety of manners (increase, decrease, and reversal of the sign of the effect), and cannot be explained by means of a simple quadratic dependence on the magnetization. The formulas for the birefringence, for example (4), were written out for the case when the effect is determined by one value of the magnetization, i.e., they can be valid for a ferromagnet or a collinear antiferromagnet. It is obvious that in the case of a more complicated magnetic structure (a two- or three-sublattice ferrimagnet), the birefringence should depend on the magnetization of all the sublattices. Thus, formula (4) can be represented in the more complicated form

$$\Delta B_{ij} = \sum_{\xi} \rho_{ijkl}^{\xi} m_k^{\xi} m_l^{\xi} + \sum_{\xi \neq \eta} \rho_{ijkl}^{\xi\eta} m_k^{\xi} m_l^{\eta}. \qquad (19)$$

In such a formulation, the first term takes into account the contribution made to the birefringence by the individual sublattices, and the second term should describe the deviations from a simple additive dependence, i.e., it should take into account the interaction of the sublattices.

The different temperature dependences of the magnetizations of the individual sublattices can lead to a complicated temperature dependence of the observed birefringence. Thus, if a large relative contribution is made by the sublattice having the stronger temperature dependence of the magnetization (for example, the rare-earth sublattice), then a lowering of the temperature can lead to a predominance of the relative contribution from this sublattice and to a change of the monotonic variation or of the sign of the summary birefringence.

The competing influence of the sublattices on the magnitude of the birefringence can be seen already from a comparison of the data for yttrium (two-sublattice structure) and rare-earth iron garnets (three and more sublattice structures). Thus, in terbium iron garnet the rare-earth sublattice decreases strongly the value of the birefringence at $\mathbf{H} \parallel [100]$ (from 125 to 45 deg/cm, Fig. 4a), leading to a reversal of the sign of the birefringence with further increase of the magnetization of the terbium sublattice.

A quantitative interpretation of the magnitude and observed temperature dependence of the birefringence must apparently be deferred for the time being until more complete field and temperature investigations are performed and a microscopic theory of this phenomenon in magnetic crystals is developed.

From the phenomenological point of view, iron garnets are an interesting example of tunable optical crystals, where the magnitude of the birefringence, the position of the optical axes, and the phase velocity of differently polarized rays can be varied in a wide range as functions of the magnetization orientation (strong birefringence anisotropy), by varying the temperature and also by using composition with different ion concentrations in the sublattices.

By way of an example let us consider the temperature variation of the parameter a and the motion of the optical axes in samarium, europium, terbium, dysprosium, and holmium iron garnets (Fig. 11). In the samarium and europium iron garnets, in which there is no magnetization compensation point, the a(T) dependence is smooth. When the external field is oriented along a twofold axis (Fig. 2), the optical axes of $Sm_3Fe_5O_{12}$ move with decreasing temperature from the $(1\bar{1}0)$ plane, which contains the magnetization **M**, to the (110) plane, which is perpendicular to **M**. The transition is through the [001] axis, so that no bire-

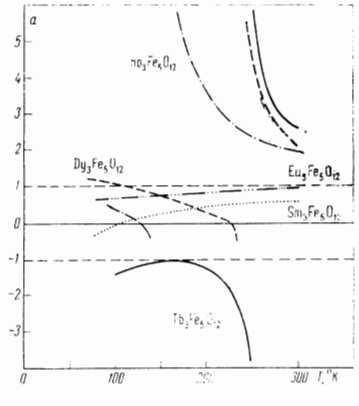

FIG. 11. Temperature behavior of the optical axes in samarium, europium, terbium, dysprosium, and holmium iron garnets when the magnetization is oriented along a twofold axis. The position of the optical axis is determined by the value of the parameter a in accord with Fig. 2.

fringence is observed at $T \sim 100°K$ for light propagating along [001] perpendicular to **M** (the Cotton-Mouton effect geometry!). A similar experiment in $Eu_3Fe_5O_{12}$ in the investigated temperature interval leads to a deflection of the optical axes from the magnetization in the $(1\bar{1}0)$ plane.

In garnets with a magnetization compensation point, the parameter a experiences a discontinuity in the region of this point and becomes infinite (Fig. 11). This shows that the optical axes in the crystals, for example in $Tb_3Fe_5O_{12}$, move on passing through T_c (Fig. 2) in the (001) plane through the [100] axis almost to the $[1\bar{1}0]$ direction. In $Ho_3Fe_5O_{12}$, a similar process takes place, but the axes move farther with decreasing temperature, and go over first into the (110) plane, which is perpendicular to **M**, and then through [001] to the $(1\bar{1}0)$ plane. In $Dy_3Fe_5O_{12}$, the optical axes execute a "complete revolution": they go over in succession from the (001) plane to the (110) plane and then to $(1\bar{1}0)$, after which they return to the (001) plane.

The authors are grateful to Corresponding Member of the USSR Academy of Sciences G. A. Smolenskiĭ for interest in the work and to N. N. Syrnikova for x-ray orientation of the crystals, and also to A. G. Titova for supplying the garnet crystals for the investigations.

[1] J. F. Dillon, Jr., J. Appl. Phys., 29, 1286 (1958).
[2] R. V. Pisarev, I. G. Siniĭ, and G. A. Smolenskiĭ, ZhETF Pis. Red. 9, 112, 294 (1969) [JETP Lett. 9, 64, 172 (1969)]; Zh. Eksp. Teor. Fiz. 57, 737 (1969) [Sov. Phys.-JETP 30, 404 (1970)].
[3] J. F. Dillon, Jr., J. P. Remeika, and C. R. Staton, J. Appl. Phys., 40, 1510 (1969).
[4] A. C. Boccara, J. Ferre, B. Briat, M. Billardon, and J. P. Badoz, J. Chem. Phys., 50, 2716 (1969).
[5] R. V. Pisarev, Zh. Eksp. Teor. Fiz. 58, 1421 (1970) [Sov. Phys.-JETP 31, 761 (1970)].
[6] L. D. Landau and E. M. Lifshitz, Élektrodinamika sploshnykh sred (Electrodynamics of Continuous Media), Gostekhizdat, 1957.
[7] V. M. Agranovich and V. L. Ginzburg, Kristallooptika s uchetom prostranstvennoĭ dispersii i teoriya éksitonov (Crystal Optics with Consideration of Spatial Dispersion, and Exciton Theory), Nauka, 1965.
[8] J. F. Nye, Physical Properties of Crystals, Clarendon Press, Oxford, 1964.
[9] R. R. Birrs, Symmetry and Magnetism, Amsterdam, 1964.
[10] R. V. Pisarev, I. G. Siniĭ, and G. A. Smolenskiĭ, Izv. Akad. Nauk SSSR, Seriya Fiz. 5, 1032 (1970); Fiz. Tverd. Tela 12, 118 (1970) [Sov. Phys.-Solid State 12, 93 (1970)].
[11] V. B. Tatarskiĭ, Kristallooptika i immersionnyĭ metod (Crystal Optics and the Immersion Method), Nauka, 1965.
[12] A. E. Clark and R. E. Strakna, J. Appl. Phys., 32, 1172 (1961).
[13] R. W. Dixon, J. Appl. Phys., 38, 5149 (1967).
[14] J. F. Dillon, Jr., J. P. Remeika, and C. R. Staton, J. Appl. Phys., 41, 4613 (1970).
[15] R. Pauthenet, Ann. Phys., Paris, 3, 424 (1958).
[16] S. Geller, J. P. Remeika, R. C. Sherwood, H. J. Williams, and G. P. Espinosa, Phys. Rev., 131, 1080 (1963); 137, A1034 (1965).
[17] R. F. Pearson, J. Appl. Phys., 33, 1236 (1962).
[18] J. J. van Loef, Solid State Commns., 6, 541 (1968).

Translated by J. G. Adashko
236